

On the Possibility of Tunable-Gap Bilayer Graphene FET

Gianluca Fiori

Dipartimento di Ingegneria dell'Informazione: Elettronica, Informatica, Telecomunicazioni,
Università di Pisa

Giuseppe Iannaccone

Dipartimento di Ingegneria dell'Informazione: Elettronica, Informatica, Telecomunicazioni,
Università di Pisa

On the Possibility of Tunable-Gap Bilayer Graphene FET

Gianluca Fiori and Giuseppe Iannaccone

Abstract—We explore the device potential of a tunable-gap bilayer graphene (BG) FET exploiting the possibility of opening a bandgap in BG by applying a vertical electric field via independent gate operation. We evaluate device behavior using atomistic simulations based on the self-consistent solution of the Poisson and Schrödinger equations within the nonequilibrium Green's function formalism. We show that the concept works, but the bandgap opening is not strong enough to suppress band-to-band tunneling in order to obtain a sufficiently large $I_{\text{on}}/I_{\text{off}}$ ratio for CMOS device operation.

Index Terms—Graphene, nonequilibrium Green's function (NEGF), tight-binding Hamiltonian.

I. INTRODUCTION

GRAPHENE HAS entered the nanoelectronics scenario only recently, and it is intensely investigated as a promising candidate to replace silicon as a channel material in nanoscale transistors. Even though graphene is a gapless material, a significant energy gap can be opened in different ways, like by “rolling” it in carbon nanotubes [1] or by defining narrow graphene stripes through electron beam lithography [2] or chemical synthesis [3]. However, several unsolved technological problems arise: State-of-the-art technology cannot indeed conveniently control the chirality and the nanotube position, as well as define graphene nanoribbons with widths close to 1–2 nm with atomically flat edges, in order to obtain an acceptable energy gap.

Recently, theoretical models [4], [5] and experiments [6]–[8] have shown that bilayer graphene (BG) has an energy gap that is controllable by a vertical electric field. One could exploit this property to use BG as a channel material for FETs, defining an energy gap only when really needed, i.e., when the FET must be in the OFF state. This capability could open the possibility of patterning a BG sheet with lithographic techniques and nonprohibitive feature sizes.

In this letter, we want to assess the possibility of realizing a tunable-gap BG-FET with independent gate operation, based

Manuscript received October 1, 2008. Current version published February 25, 2009. This work was supported in part by the EC Seventh Framework Program under Project GRAND (Contract 215752), by the Network of Excellence NANOSIL (Contract 216171), and by the European Science Foundation EUROCORES Programme Fundamentals of NanoElectronics, through funds from CNR and the EC Sixth Framework Program, under Project DEWINT (Contract ERAS-CT-2003-980409). The review of this letter was arranged by Editor J. Cai.

The authors are with the Dipartimento di Ingegneria dell'Informazione: Elettronica, Informatica, Telecomunicazioni, Università di Pisa, 56126 Pisa, Italy (e-mail: g.fiori@iet.unipi.it).

Digital Object Identifier 10.1109/LED.2008.2010629

on atomistic numerical simulations. We assume that all the technological challenges associated to the reliable fabrication of BG-FETs can be solved, and we evaluate the potential performance of near-ideal device structures. In our opinion, this is one of the most powerful uses of computer simulations in guiding and orienting nanoelectronics research.

Numerical simulations based on the nonequilibrium Green's function formalism (NEGF) within the effective mass approximation have been presented [9] in order to compare bilayer graphene transistors against monolayer ones. That work, while giving a qualitative understanding of graphene bilayer FET performance and catching its main limitations, assumes a constant induced energy bandgap and effective mass for BG, missing important properties of the material.

For a physically sound analysis of BG-FETs, we have developed a code based on the NEGF, with a tight-binding Hamiltonian on a p_z orbital basis set in the real space, which has been included in our in-house open-source device simulator NANOTCAD ViDES [10].

We will show that BG-FETs miss the ITRS requirements [11] for the $I_{\text{on}}/I_{\text{off}}$ ratio ($> 10^4$) by a large amount, since the induced gap is not sufficient to suppress band-to-band tunneling currents.

II. PHYSICAL MODEL AND RESULTS

Our approach is based on the self-consistent solution of the Poisson and Schrödinger equations within the NEGF formalism and the ballistic transport assumption, as described in [12]. The considered BG Hamiltonian is composed by two single-layer graphene Hamiltonians, coupled by the hopping parameter $t_p = 0.35\text{-eV}$ in correspondence of the overlaying atoms along the z -direction [5]: The elementary cell [Fig. 1(a)] is repeated periodically along the x - and y -directions. In particular, Bloch-periodic boundary conditions are imposed along the x -direction with period that is equal to $\Delta = \sqrt{3}a_{\text{cc}}$, where $a_{\text{cc}} = 0.144\text{ nm}$ is the carbon-carbon bonding distance. In this way, the k_x wave vector appears in the Hamiltonian. Semi-infinite contacts have been instead modeled along the y -direction by means of self-energies.

The simulated device is a double-gate BG-FET, whose structure is shown in Fig. 1(b). We assume metal gates, and a 1.5-nm layer of SiO_2 as gate dielectric. We also assume an air gap of 0.5 nm between the dielectric interface and the position of carbon sites, as evaluated in [3]. The channel is 15 nm long, and the interlayer distance is 0.35 nm. The source and drain extensions are 10 nm long and are doped with an equivalent molar fraction of fully ionized donors $f_d = 5 \times 10^{-3}$.

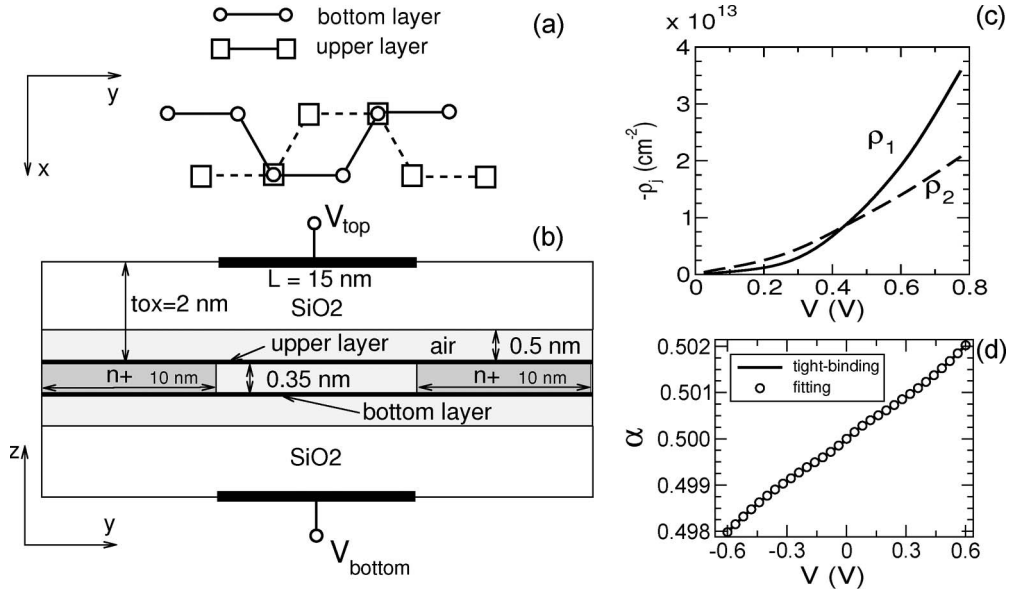


Fig. 1. (a) Elementary cell of the simulated BG. (b) Transversal cross section of the simulated graphene bilayer field-effect transistor. (c) Electron density computed as in (1) (solid line) on the top and (dashed line) on the bottom layer as a function of the potential V imposed on the bilayer. (d) (Solid line) Tight-binding and (symbols) least mean squares fitting analytical results for the polarization factor α in (2).

Particular attention has to be posed in the computation of the mobile charge. Considering, for the sake of simplicity, the equilibrium case, the mobile charge on a given site on layer j ($j = 1, 2$) of the BG sheet reads

$$\rho_j = -2q \int_{-\frac{\pi}{\Delta}}^{\frac{\pi}{\Delta}} \int_{E_i}^{+\infty} dk_x dE LDOS_j(E, k_x, V) f(E) + 2q \int_{-\frac{\pi}{\Delta}}^{\frac{\pi}{\Delta}} \int_{-\infty}^{E_i} dk_x dE LDOS_j(E, k_x, V) [1 - f(E)] \quad (1)$$

where q is the elementary charge, E_i is the intrinsic (midgap) Fermi level, f is the Fermi-Dirac occupation factor, $LDOS_j(E, k_x, V)$ is the local density of states on layer j , V is the potential difference between the top and the bottom layer, and the integral on k_x is performed on the Brillouin zone $-\pi/\Delta \leq k_x \leq \pi/\Delta$.

Let us stress the fact that in order to avoid an unphysical antiscreeing behavior, it is necessary to include the effect of dielectric polarization along the direction perpendicular to the graphene bilayer, due to the response of valence electrons to the applied field. Indeed, as shown in Fig. 1(c), the charge computed as in (1), shows an unphysical larger accumulation of electrons on the bottom layer (ρ_2 , dashed line), rather than on the top layer (ρ_1 , solid line), when V is smaller than 0.4 V.

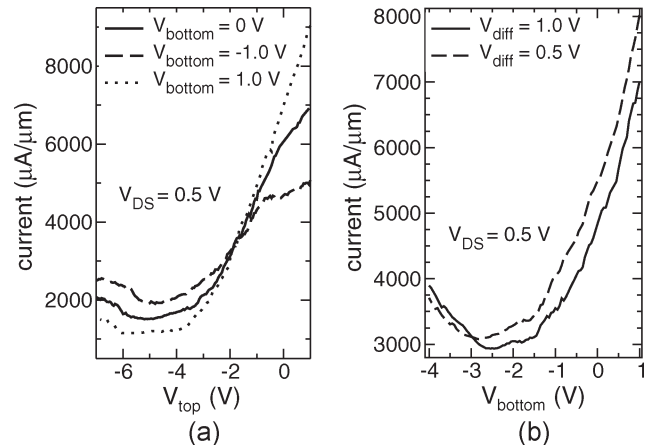


Fig. 2. (a) Transfer characteristics computed as a function of the top gate voltage, when the (dotted line) bottom gate voltage $V_{\text{bottom}} = 1.0$ V, (solid line) $V_{\text{bottom}} = 0$ V, and (dashed line) $V_{\text{bottom}} = -1.0$ V. (b) Transfer characteristics computed as a function of V_{bottom} for (solid line) $V_{\text{diff}} = 1.0$ V and (dashed line) $V_{\text{diff}} = 0.5$ V.

To include the polarization of valence-band electrons in a computationally effective way, we introduce a polarization factor α defined as (2) and shown at the bottom of the page.

By using α , we can write the total charge (mobile charge, valence-band electrons, and ions) on a given site of layers 1 and 2 as

$$\begin{aligned} \rho'_1 &= \rho_1 + q[1 - 2\alpha(V)] \\ \rho'_2 &= \rho_2 - q[1 - 2\alpha(V)]. \end{aligned} \quad (3)$$

$$\alpha(V) = \frac{\int_{-\frac{\pi}{\Delta}}^{\frac{\pi}{\Delta}} \int_{-\infty}^{E_i} LDOS_1(E, k_x, V) dE dk_x}{\int_{-\frac{\pi}{\Delta}}^{\frac{\pi}{\Delta}} \int_{-\infty}^{E_i} [LDOS_1(E, k_x, V) + LDOS_2(E, k_x, V)] dE dk_x} \quad (2)$$

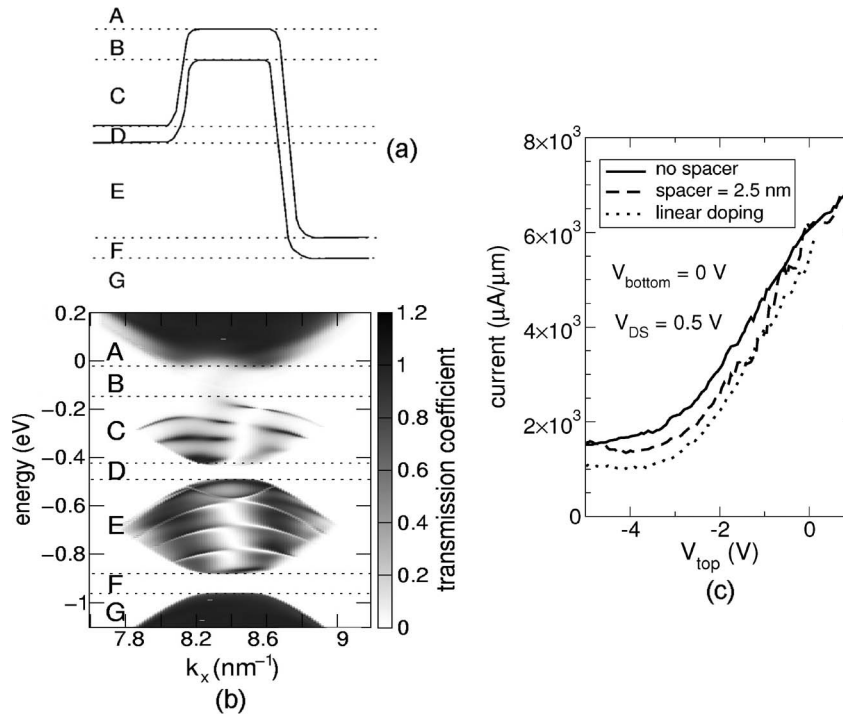


Fig. 3. (a) Sketch of the band-edge profile. (b) Transmission coefficient as a function of the energy and the transversal wave vector k_x for $V_{\text{bottom}} = 0$ V, $V_{\text{top}} = -4.0$ V, and $V_{\text{DS}} = 0.5$ V. (c) Transfer characteristics for a BG-FET with 2.5-nm spacer and a BG-FET with doping profile linearly varying over a 25-nm-long region from zero to f_d .

However, performing the integral from $-\infty$ to E_i in (2) at each iteration step can be too computationally demanding. For this purpose, we compute the polarization factor as a function of V only once, for an infinitely long BG-FET [solid line in Fig. 1(d)]. As can be seen, $\alpha(V)$ can be reasonably approximated by a straight line $\alpha(V) = 0.5 + 3.282 \times 10^{-3} V$. In our code, we have used an odd polynomial of 11th order obtained through least mean squares fitting [symbols in Fig. 1(d)].

In Fig. 2, the transfer characteristics for $V_{\text{DS}} = 0.5$ V are shown, for different gate configurations. In particular, in Fig. 2(a), the transfer characteristics as a function of the top gate voltage V_{top} for different gate voltages are shown. As can be seen, large currents can be obtained above threshold, while the BG-FET shows huge problems to switch off. Even after applying very negative gate voltages, the drain-to-source current decreases only by roughly a factor of six. The ratio even worsens when $V_{\text{bottom}} = -1.0$ V, since, in this case, a larger amount of positive charge is injected in the valence band, due to band-to-band tunneling, which pins the potential along the channel, and further degrades the gate control over the barrier.

Such results are close to those obtained in experiments on monolayer graphene devices [13], showing that the tunable gap is too small to effectively suppress band-to-band tunneling in the OFF state.

In order to increase the vertical electric field between the two layers of graphene, we have driven the device by imposing a fixed voltage between the two gates $V_{\text{diff}} = V_{\text{top}} - V_{\text{bottom}}$.

Even in this case, device transconductance (i.e., the slope of the transfer characteristic) remains almost the same, regardless of the applied V_{diff} . This can be explained by the large accu-

mulation of positive charge in the channel, which is caused by band-to-band tunneling in correspondence of the drain [12]: This charge screens the vertical electric field, limiting the size of the opened bandgap.

In Fig. 3(b), the transmission coefficient as a function of the transversal wave vector k_x is shown for $V_{\text{top}} = -4.0$ V, $V_{\text{DS}} = 0.5$ V, and $V_{\text{bottom}} = 0$ V, i.e., close to the minimum achievable current, and in correspondence of the band minimum. Different energy intervals are identified with letters and compared to a sketch of the band-edge profile in Fig. 3(a) as an aid to interpretation. As can be seen, energy intervals tagged as B, D, and F correspond to the bandgaps in the channel, source, and drain extensions, respectively: The gap is not uniform, and it is maximum in the channel, where it is almost 100 meV. One can also see the bound states in the valence band in the energy interval C and the valence-band states in E, which are populated by holes for negative voltages, and which eventually pin the potential of two monolayers of graphene, i.e., reducing the gate effectiveness in controlling the channel barrier and the bandgap.

Band-to-band tunneling can, in principle, be reduced by engineering the electric field between the source and the channel. Here, we make two attempts, i.e., by introducing a lateral spacer on the gate sides of 2.5 nm and by introducing a linear doping profile degrading from f_d to zero in 25 nm along the doped reservoirs. Both options have a positive but limited effect, as shown in Fig. 3(c), and do not solve the problem.

III. CONCLUSION

We have explored the possibility of realizing FETs by exploiting the tunable-gap property of BG, through a code

based on tight-binding NEGF device simulations. Aiming at technology foresight, we have considered the overly optimistic case of an ideal structure and of ballistic transport.

Our computer simulations show that tuning the gap is not a very promising technique for achieving appropriate switching characteristics of BG-FETs, due to the too weak suppression of band-to-band tunneling. A more complete exploration of the design space, in terms of structure and bias, would be required to cast a definitive answer, which is beyond the scope of this letter.

ACKNOWLEDGMENT

The authors would like to thank the Network for Computational Nanotechnology for providing computational resources at nanohub.org through which part of the results shown here has been obtained.

REFERENCES

- [1] S. Iijima, "Helical microtubules of graphite carbon," *Nature*, vol. 354, no. 6348, pp. 56–58, Nov. 1991.
- [2] Z. Chen, Y.-M. Lin, M. J. Rooks, and P. Avouris, "Graphene nano-ribbon electronics," *Phys. E*, vol. 40, no. 2, pp. 228–232, Dec. 2007.
- [3] X. Li, X. Wang, L. Zhang, S. Lee, and H. Dai, "Chemically derived, ultrasmooth graphene nanoribbon semiconductors," *Science*, vol. 319, no. 5867, pp. 1229–1232, Feb. 2008.
- [4] E. McCann and V. I. Fal'ko, "Landau-level degeneracy and quantum Hall effect in a graphite bilayer," *Phys. Rev. Lett.*, vol. 96, no. 8, p. 086 805, Mar. 2006.
- [5] J. Nilsson, A. H. Castro Neto, F. Guinea, and N. M. R. Peres, "Electronic properties of graphene multilayers," *Phys. Rev. Lett.*, vol. 97, no. 26, p. 266 801, Dec. 2006.
- [6] E. V. Castro, K. S. Novoselov, S. V. Morozov, N. M. R. Peres, J. M. B. Lopes dos Santos, J. Nilsson, F. Guinea, A. K. Geim, and A. H. Castro Neto, "Biased bilayer graphene: Semiconductor with a gap tunable by the electric field effect," *Phys. Rev. Lett.*, vol. 99, no. 21, p. 216 802, Nov. 2007.
- [7] T. Ohta, A. Bostwick, T. Seyller, K. Horn, and E. Rotenberg, "Controlling the electronic structure of bilayer graphene," *Science*, vol. 313, no. 5789, pp. 951–954, Aug. 2006.
- [8] J. B. Oostinga, H. B. Heersche, X. Liu, and A. F. Morpurgo, "Gate-induced insulating state in bilayer graphene devices," *Nat. Mater.*, vol. 7, no. 2, pp. 151–157, Feb. 2008.
- [9] Y. Ouyang, P. Campbell, and J. Guo, "Analysis of ballistic monolayer and bilayer graphene field-effect transistors," *Appl. Phys. Lett.*, vol. 92, no. 6, p. 063 120, Feb. 2008.
- [10] See the website for the source code and the documentation. [Online]. Available: <http://www.nanohub.org/tools/vides>
- [11] *International Technology Roadmap for Semiconductor 2007*. [Online]. Available: <http://public.itrs.net>
- [12] G. Fiori, G. Iannaccone, and G. Klimeck, "A three-dimensional simulation study of the performance of carbon nanotube field-effect transistors with doped reservoirs and realistic geometry," *IEEE Trans. Electron Devices*, vol. 53, no. 8, pp. 1782–1788, Aug. 2006.
- [13] M. C. Lemme, T. J. Echtermeyer, M. Baus, and H. Kurz, "A graphene field-effect device," *IEEE Electron Device Lett.*, vol. 28, no. 4, pp. 282–284, Apr. 2007.
- [14] G. Fiori and G. Iannaccone, "Simulation of graphene nanoribbon field-effect transistors," *IEEE Electron Device Lett.*, vol. 28, no. 8, pp. 760–762, Aug. 2007.